Available online at www.sciencedirect.com

ScienceDirect

journal homepage: www.elsevier.com/locate/he

Design tool for estimating adsorbent hydrogen storage system characteristics for light-duty fuel cell vehicles

Carina Grady [a,*], *Scott McWhorter* [a], *Martin Sulic* [b], *Samuel J. Sprik* [c], *Matthew J. Thornton* [c], *Kriston P. Brooks* [d], *David A. Tamburello* [a]

[a] *Savannah River National Laboratory, Aiken, SC, USA*
[b] *Oak Ridge Institute for Science and Education, Washington, DC, USA*
[c] *National Renewable Energy Laboratory, Golden, CO, USA*
[d] *Pacific Northwest National Laboratory, Richland, WA, USA*

HIGHLIGHTS

- Model analysis of adsorption-based hydrogen system for fuel cell applications.
- Evaluation of various engineering design options for tank and balance-of-plant.
- Thermodynamic equations to predict charging/discharging of activated carbon and MOF-5.
- Prototype validation and model sensitivity analysis for data comparison.
- Full-vehicle level analysis compared to DOE standards to determine applicability.

GRAPHICAL ABSTRACT

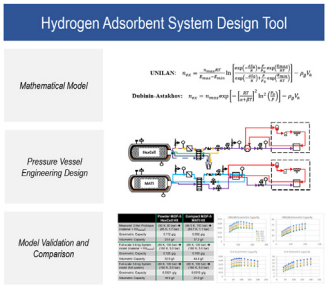

ARTICLE INFO

Article history:
Received 6 January 2022
Received in revised form
14 June 2022
Accepted 27 June 2022
Available online 20 August 2022

Keywords:
Fuel cell vehicle
Adsorbent hydrogen storage

ABSTRACT

This work combines materials development with hydrogen storage technology advancements to address onboard hydrogen storage challenges in light-duty vehicle applications. These systems are comprised of the vehicle requirements design space, balance of plant requirements, storage system components, and materials engineering culminating in the development of an Adsorbent System Design Tool that serves as a preprocessor to the storage system and vehicle-level models created within the Hydrogen Storage Engineering Center of Excellence. Computational and experimental efforts were integrated to evaluate, design, analyze, and scale potential hydrogen storage systems and their supporting components against the Department of Energy 2020 and Ultimate Technical Targets for Hydrogen Storage Systems for Light Duty Vehicles. Ultimately, the Adsorbent System

* *Corresponding author.*
E-mail address: carina.grady@srnl.doe.gov (C. Grady).
https://doi.org/10.1016/j.ijhydene.2022.06.281
0360-3199/Published by Elsevier Ltd on behalf of Hydrogen Energy Publications LLC.

MOF-5
System model

Design Tool was created to assist material developers in assessing initial design parameters that would be required to estimate the performance of the hydrogen storage system once integrated with the full fuel cell system.

Introduction

The Department of Energy (DOE) has heavily invested in the future of green energy over the years, including the commercialization of hydrogen-powered fuel cell electric vehicles. The DOE has published specific technical targets [1] for hydrogen fuel cell vehicles to make them competitive with modern gasoline/diesel vehicles with driving ranges approaching 500 miles. While there are several barriers to the widespread use of hydrogen-powered vehicles, one of the more technically challenging aspects involves the on-board hydrogen storage.

There are six methods of on-board hydrogen storage that can be broken into two overarching categories: thermodynamic storage and material-based storage. Thermodynamic storage uses changes in pressure and/or temperature to increase hydrogen storage and is typically categorized based on the operating temperature: room temperature compressed (~298 K), cryogenic temperature (~77 K), cryo-compressed (CcH_2), and liquid hydrogen storage [2]. Note that there is also a sub-category of thermodynamic storage sometimes called cold storage that typically refers to dry ice or 200 K temperature range. While these thermodynamic storage methods have had some success in light-duty vehicle (LDV) applications [3], they still do not meet the DOE technical targets. The second overarching category of hydrogen storage is material-based storage, which includes chemical hydrogen storage [4–6] that have the strongest hydrogen bonds but require off-board regeneration, metal hydrides [7–9], which can be refueled on-board and undergo chemical reactions during the charging process, and adsorbents [10–14] which use reversible physisorption mechanisms to store hydrogen and is the material-based hydrogen storage method discussed in this paper.

Each of these material-based hydrogen storage methods show promise in on-board vehicle storage, but no one material can meet the DOE technical targets. For this reason, the DOE sponsored the HSECoE, which was tasked with developing engineering solutions for enabling material-based hydrogen storage on-board LDVs. This work involved identifying, developing, and experimentally evaluating critical components of the hydrogen storage systems on a bench scale. In short, the HSECoE was tasked with bridging the gap between the mg-scale of hydrogen storage research in the laboratory and kg-scale on-board hydrogen storage needs of LDVs. Computational models and other toolsets were created for the hydrogen storage materials research community that are available in the public domain [15]. One of the more notable computational tools available are the detailed finite element analyses (FEA) models of adsorbent storage systems [14,16] that show the interactions with adsorbent-specific heat exchanger designs and the need for specific balance of plant (BOP) components. Arguably the most useful computational tool, and the primary subject of this paper, is the adsorbent system design tool (ASDT) developed to help materials researchers use their laboratory-scale excess adsorption data to design full-scale hydrogen storage systems for LDVs.

System design tools, such as the ASDT, are necessary for comparing various hydrogen storage materials under consistent conditions, especially when scaling laboratory material measurements to full scale automotive systems [1]. Several studies have been done to estimate system level performance from excess adsorption laboratory measurements [17,18]. Tamburello et al. [19] used an early version of the ASDT to compare various operating conditions, material properties, heat exchanger designs, and overall full system designs to estimate the useable hydrogen storage capacities of various AX-21 and MOF-5™ based systems. They showed that there are trade-offs in system design considerations, as well as that the adsorbent when the highest total hydrogen storage does not necessarily result in the greatest useable system-level hydrogen storage capacity. One such trade-off is the decision to use powder adsorbents versus densified pellets to increase hydrogen storage capacity [20,21]. And while densifying an adsorbent does increase its volumetric capacity, these studies show a decrease in gravimetric capacity and a reduction in overall adsorption efficiency as some of the adsorption sites can be damaged during densification. Many researchers have attempted to increase adsorption capacity [22], but no adsorbent has been able to meet the DOE technical targets [1].

Ultimately, the ASDT was created to assist material developers in assessing initial design parameters that would be required to estimate the performance of the hydrogen storage system once integrated with the full fuel cell system to discover which materials show the most promise to meet the DOE technical targets. The present article described the development and utility of the ASDT both as a stand-alone design tool and as a preprocessor to the storage system and vehicle-level models described in earlier works [23,24]. As a stand-alone design tool, the ASDT allows adsorbent material developers to estimate the total system mass and volume for the full-scale LDV, as well as the mass and size of the individual components that make up the hydrogen storage system. The materials developer can also examine effects of changes in operating conditions to better tune their specific adsorbent and find its optimum storage conditions. This ASDT tool can be used as an initial test of a new adsorbent material or for parametric analyses [19] to make design decisions for use in building adsorbent storage prototypes, such as those tested at the conclusion of the HSECoE. An ASDT

was created to assist material developers in making estimates for initial design parameters that would then be used as inputs into a broader vehicle framework model to estimate the performance of the H_2 storage system integrated with the fuel cell system. The tool provides an estimate of the total system mass and volume, as well as the size of the individual components that feed into both the fuel cell and total LDV framework model. Additionally, the ASDT estimates the control parameters required for a particular H_2 storage material. This paper describes the utility of the validated adsorption-based H_2 storage system models. This information can be used for parametric analyses and system design decisions for use in building adsorbent storage prototypes, such as those tested at the conclusion of the HSE-CoE. In summary, this tool is meant to bridge the gap between the thermodynamic and kinetic information generally measured by H_2 storage material developers and the information required to exercise the broader fuel cell LDV Framework model.

Adsorbent hydrogen storage system design

For adsorbent-based H_2 storage systems, two types of tank designs are identified that adsorb and desorb H_2: HexCell and MATI, which are further discussed in detail in Sections HexCell System Design for Powdered Adsorbents and MATI System Design for Compacted Adsorbents, respectively. These designs were selected as the top-yielding result from a comprehensive parametric study that paired variations on adsorbent material, packing densities, internal heat exchanger, pressure vessel (PV) type, and more. Details of this parametric analysis can be found in a 2017 conference paper by Tamburello et al. [19]. Both designs assume that the adsorbent has a reasonable thermal conductivity for appropriate heat transfer. Table 1 outlines key differences between the two storage system designs.

In short, both storage system designs utilize liquid nitrogen chilling to store energy from refueling, and heating to release energy from defueling to the fuel cell. The layers of the tank are also the same for both designs, as seen in Fig. 1. There are five layers total, ordered from the inner to outer walls of the tank: metal liner, carbon fiber layer (Type 3 and 4 tanks, if applicable), liquid nitrogen chilling channel (if applicable), multilayer vacuum insulation (MLVI) in evacuated space, and the outer vacuum shell.

Table 1 – Storage system design specifications.

	HexCell	MATI
Pressure vessel operating pressure [MPa]	0.5–10	0.5–10
Pressure vessel operating temperature [K]	80–140	80–140
$H_{2,useable}$ [kg]	5.6	5.6
Internal tank volume [L]	188.4	180.1
Tank L-to-D ratio	2:1	2:1
Aluminum PV thickness [mm]	14.00	13.06
MLVI thickness [mm]	25.4	25.4
Outer Al shell thickness [mm]	2.0	2.0
Total system mass [kg]	140.99	141.59
Total system volume [L]	287.70	246.03
Total system cost[a]	$2219	$2616
System Gravimetric Capacity [$g_{H2,useable}/g_{system}$]	0.03974	0.03957
System Volumetric Capacity [$g_{H2,useable}/L_{system}$]	19.47	22.77

[a] System costs are estimates for system-to-system comparison purposes only and not intended to represent the actual market cost of these systems.

HexCell system design for powdered adsorbents

The internal heat exchanger design, nicknamed the HexCell, includes longitudinal hexagonal-shaped tubes to be packed with powder adsorbent material, lanced to ensure maximum cross-sectional area H_2 flow. Fig. 2 displays a fueling and refueling schematic associated with the HexCell system design.

H_2 flows through the fill receptacle, travels through the separation valve, and is absorbed in the HexCell tank. After the adsorbed H_2 in the tank reaches the set pressure (typically the full system pressure of 10 MPa), a solenoid valve opens to allow flow-through H_2 to leave the system. This flow-through H_2 travels past safety valves, pressure/temperature sensors, and a separation valve before returning to the refueling receptacle where it is cooled for the next round of refueling. This is all done while maintaining the pressure of the tank even as the temperature begins to decrease. Although this method will reach the desired temperature and pressure required to maximize the adsorption in the tank, a considerable amount of costly H_2 is needed for absorption and to pressurize and cool the tank.

To minimize the amount of required H_2, a liquid nitrogen stream is introduced to expedite the cooling process. Because the H_2 is absorbed by the adsorbent and pressurized into a fixed volume tank, the heat of adsorption and heat of pressurization must be accounted for during the cooling process. As depicted in Fig. 2, the liquid nitrogen flows from the fueling receptacle, to the specialized cooling channels within the tank, and back to the refueling receptacle. The liquid nitrogen only flows through the vessel wall chilling channel located between the PV walls and the MLVI, purposely designed so it would boil and increase heat transfer to the surface of the tank.

With both the H_2 flow-through cooling and liquid nitrogen stream, the contents of the tank will maintain its set refueling maximum pressure (typically 10 MPa) and reach a full tank temperature (typically 80 K for cryogenic operation). Although these full tank operating conditions are adsorbent-dependent, the conditions of 80 K and 10 MPa are typical for many adsorbents, including activated carbon and MOF-5™.

Once the contents of the tank have reached quasi-steady state at the full tank conditions, H_2 is released to the fuel cell. The release/desorption of H_2 is an endothermic process that requires heat to break bonds, cooling the bulk of tank while also resulting in a lower pressure. As a result of the endothermic nature of desorption, less H_2 would be desorbed as the tank temperature drops, requiring added heat to maintain the process. Thus, electric heating rods are placed in several hexagonal slots to facilitate the desorption process, whereby H_2 leaves the tank, passing through the solenoid and safety valves.

A typical fuel cell accepts H_2 at temperatures between 233 K and 353 K (−40 °C and 80 °C). To increase the

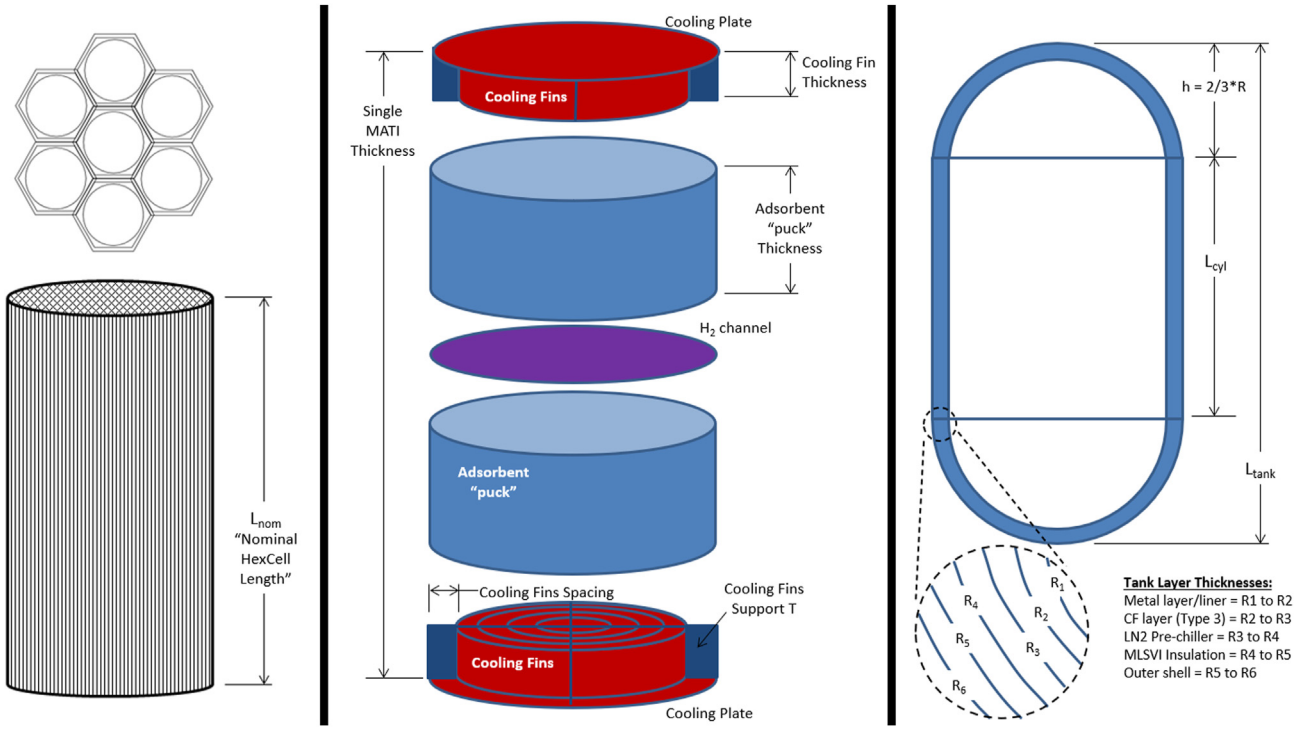

Fig. 1 – HexCell system design, MATI system design, MLVI layers.

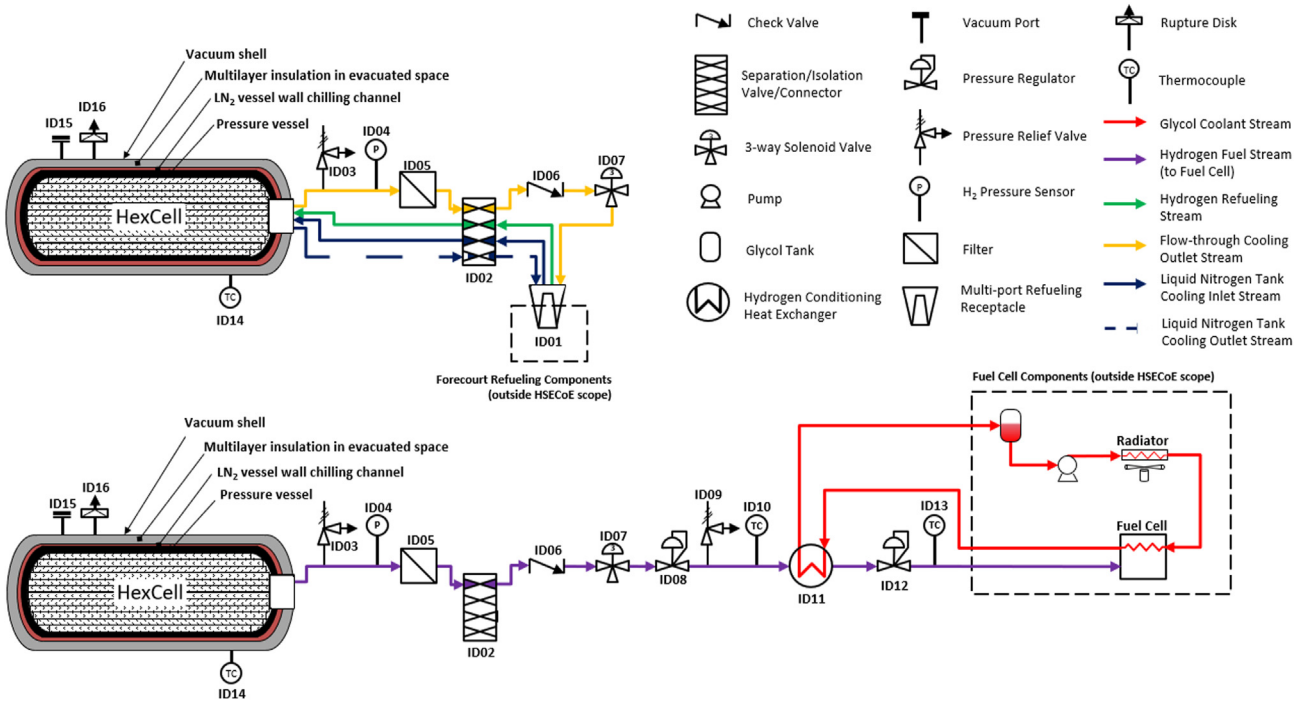

Fig. 2 – HexCell system diagram: Type 1 aluminum PV with powder MOF-5™ in a hexagonal channel flow-through cooling HX with rod resistance heaters. Top half includes refueling and bottom half includes defueling.

temperature of the incoming H_2 into the fuel cell, a compact shell-and-tube heat exchanger with a glycol-water stream is introduced. The glycol-water stream is the heat transfer fluid used in vehicle radiators to cool the fuel cell. After the H_2 undergoes the necessary heat transfer to reach an acceptable temperature between 233 K and 353 K, the stream passes through one last safety valve before entering the fuel cell.

MATI system design for compacted adsorbents

A disadvantage of a system design that relies on packed powder adsorbent is the difficulty of packing the adsorbent into thin hexagonal rods, especially when the rod material is brittle in the lateral direction. One solution is to incorporate solid adsorbent "pucks" (Fig. 3) that stack on top of one another instead. The Modular Adsorbent Tank Insert (MATI) utilizes this concept with a micro-channel isolated-fluid heat exchanger. Fig. 4 displays a fueling and refueling schematic associated with the MATI system design.

Like the HexCell system design, H_2 enters the MATI tank from the refueling receptacle. Heat of absorption and pressurization occurs, but after the tank pressure increases to the desired state, temperature decreases with the use of a liquid nitrogen cooling stream. The liquid nitrogen stream starts at the vessel wall chilling channel, and then flows into the MATI heat exchanger within the PV. These two streams return to the fuel receptacle to complete the cooling cycle. Depending on the economics, this exiting nitrogen may either be re-liquified or vented to the atmosphere.

After the contents of the tank reach the full tank temperature and pressure, the H_2 is ready to travel to the fuel cell. As H_2 is desorbed and exits the tanks, the temperature of the contents of the tank decreases due to depressurization and the endothermic process. This is offset with a H_2 heating stream that exits the tank, travels through the glycol-water heat exchanger, and returns to the tank. As H_2 from a different line exits the tank to flow towards the fuel cell, it passes through a glycol-water heat exchanger similar to the HexCell design so that the H_2 temperature can be brought to a range between 233 K and 353 K before reaching the last safety valves and fuel cell.

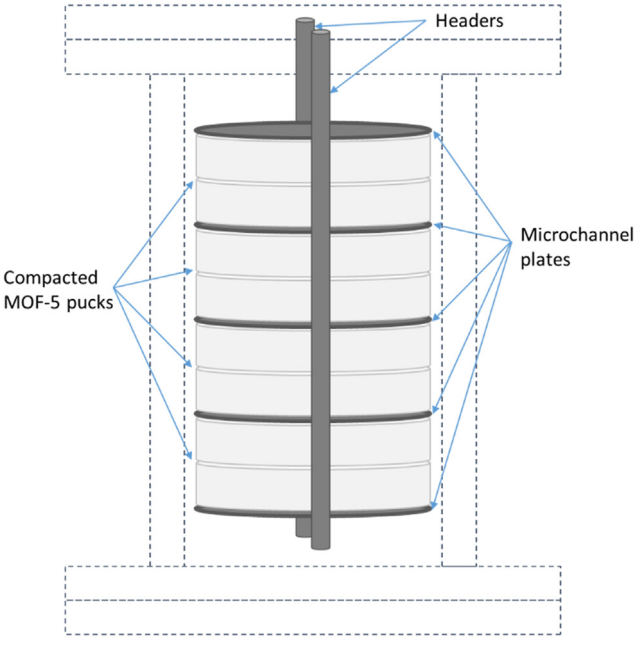

Fig. 3 – Schematic of a generic MATI internal heat exchanger within a PV.

Materials and methods

UNILAN model

Adsorption theory equations are used to simulate the gas-solid interactions in adsorption-based H_2 storage systems. While there are many different adsorption theories, a specific adsorbent can be described or modeled with a better fit using one theory versus another. Based on experience with modeling adsorbents at Savannah River National Laboratory, UNILAN is seen as one of the more versatile theory for modeling excess adsorption in H_2 storage applications [25]. Thus, the UNILAN model as described by Bhatia and Myers [26] was specifically chosen to predict the hydrogen adsorption isotherms for the materials chosen for storage system within the vehicle model. The excess adsorption equation is given below:

$$n_{ex} = n_a + \rho_g V_a \tag{1}$$

where n_{ex} is the excess adsorption, ρ_g is the bulk gas density, and V_a is the adsorption volume.

The isotherm model applies to gas within the pore volume and includes the adsorbed and free gas phases. The adsorption volume is the pore volume within a homogeneous region of adsorbent, which is assumed to be representative of an adsorbent particle. Although V_a is obtained from a regression fit to data, the variable approximates the void volume within a particle. Using the UNILAN method, the absolute adsorption is given as followed:

$$n_a = \frac{n_{max}}{2s} \ln\left[\frac{1 + K_h P e^{s}}{1 + K_h P e^{-s}}\right] \tag{2}$$

where n_{max} is the maximum adsorption coverage when the entire adsorption volume is filled, and P is pressure.

Due to the complexity of the UNILAN method, the absolute adsorption equation is broken down by variables K_h, $-\Delta\overline{H}_0$, and s, defined as followed:

$$K_h = \frac{\exp\left(\frac{\Delta S_0}{R} + \frac{-\Delta H_0}{RT}\right)}{P_0} \tag{3}$$

$$-\Delta\overline{H}_0 = \frac{E_{max} + E_{min}}{2} \tag{4}$$

$$s = \frac{E_{max} - E_{min}}{2RT} \tag{5}$$

where ΔS_0 is the entropy change relative to a standard pressure of P_0, ΔH_0 is the isosteric heat, R is the gas constant, T is temperature, E_{max} is the maximum isosteric heat value, and E_{min} is the minimum isosteric heat value.

Substituting Equations (2)–(5) into Equation (1) results in the following simplified excess adsorption equation that can be integrated into the given H_2 storage system model:

$$n_{ex} = \frac{n_{max} RT}{E_{max} - E_{min}} \ln\left[\frac{\exp\left(-\frac{\Delta S_0}{R}\right) + \frac{P}{P_0}\exp\left(\frac{E_{max}}{RT}\right)}{\exp\left(-\frac{\Delta S_0}{R}\right) + \frac{P}{P_0}\exp\left(\frac{E_{min}}{RT}\right)}\right] - \rho_g V_a \tag{6}$$

Note that P_0, n_{max}, V_a, ΔS_0, E_{min}, and E_{max} are data fitting parameters for the UNILAN theory of adsorption. The H_2

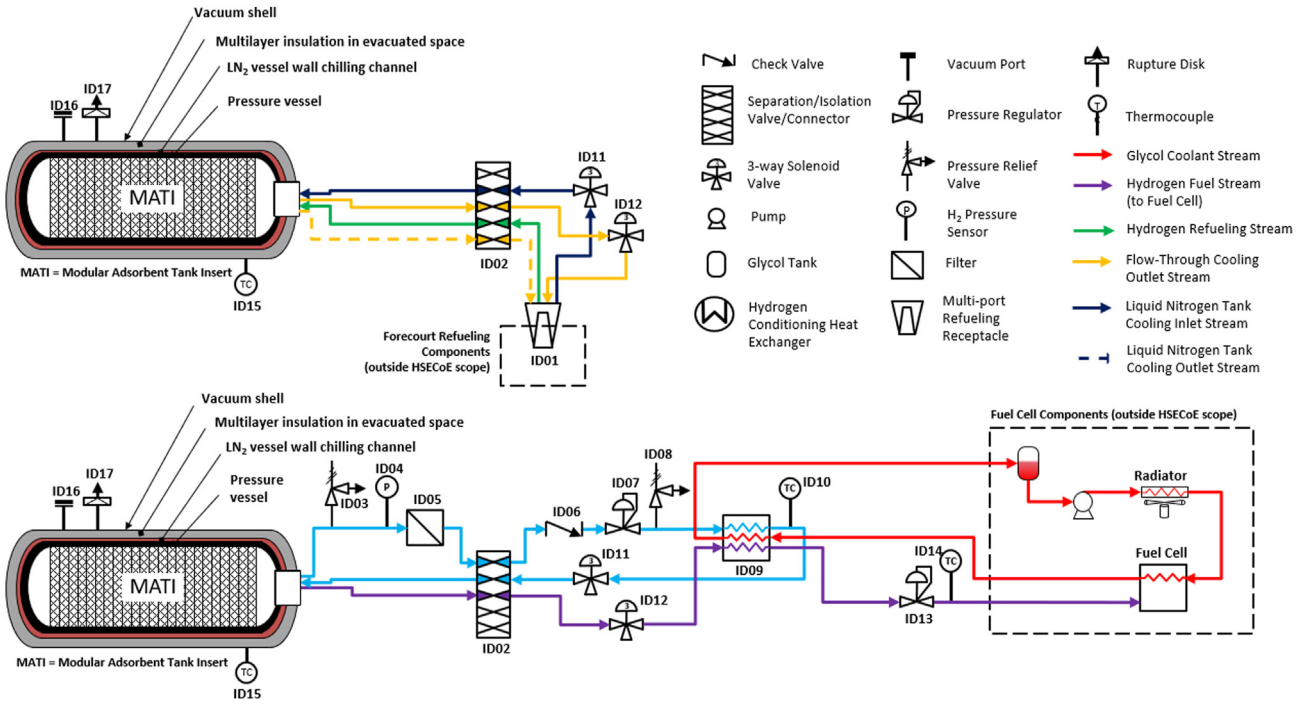

Fig. 4 – MATI system diagram: Type 1 aluminum PV with compacted MOF-5™ pucks in a microchannel isolated-fluid HX system. Top half includes refueling and bottom half includes defueling.

adsorption isotherm data originated from the following references [27–30]. Additional adsorption isotherm data from other references [31–33] were used to corroborate the data used to find the fitting parameters. Although the isosteric heat of adsorption ($\Delta\overline{h}_a^0$) is fitted into the model, it can also be calculated, as shown below:

$$\Delta\overline{h}_a^0 = -RT^2\left[\frac{\partial lnP}{\partial T}\right]_{n_a,V} = \frac{n_a(E_{max}-E_{min})}{n_{max}} + \frac{E_{min}\exp\left(\frac{E_{min}}{RT}\right) - E_{max}\exp\left(\frac{E_{max}}{RT}\right)}{\exp\left(\frac{E_{max}}{RT}\right) - \exp\left(\frac{E_{min}}{RT}\right)} \quad (7)$$

D-A model

An alternative computational approach for adsorption is the Dubinin-Astakhov (D-A) methodology. This is another useful adsorption theory that has been used extensively for activated carbon and similarly behaving adsorbent materials [11]. Because both UNILAN and D-A utilize data fitting, the excess adsorption Equation (1) is the same. However, the absolute adsorption function changes to the following:

$$n_a = n_{max}exp\left[-\left[\frac{RT}{\varepsilon}\right]^m ln^m\left(\frac{P_0}{P}\right)\right] \quad (8)$$

where n_{max}, ε, and P_0 are fitting parameters for the pressure and temperature of the experimental data. A special version of the D-A model, called the Dubinin-Radushkevich equation, is used for the ease of conversion and manipulation. In this special case, m is set to 2 instead of a fitting parameter. Using the temperature-adsorption trends showed in Czerny et al. [12], the characteristic free energy of adsorption, ε, is given by:

$$\varepsilon = \alpha + \beta T \quad (9)$$

where the enthalpic and the entropic factors are, respectively, α and β.

Experimentally measured excess adsorption isotherms can then be fit to the following equation formed from Equations (1), (8) and (9):

$$n_{ex} = n_{max}exp\left[-\left[\frac{RT}{\alpha+\beta T}\right]^2 ln^2\left(\frac{P_0}{P}\right)\right] - \rho_g V_a \quad (10)$$

where n_{max}, α, β, P_0, and V_a are the fitting parameters.

Like Equation (7), the isosteric heat of adsorption can be calculated from the preceding equations, but the more common form is provided by Myers and Monson [34]:

$$\Delta\overline{h}_a^0 = -RT^2\left[\frac{\partial lnP}{\partial T}\right]_{n_a,V} = -\alpha\sqrt{-ln\left(\frac{n_a}{n_{max}}\right)} \quad (11)$$

Model options

Knowing the engineering system design and the computational isotherm fitting, a model may be created. To set up the model, various information would have to be considered first, with the bulk of the options listed in Table 2. Note that these options are available for the model regardless of the adsorbent isotherm modeling platform (i.e., UNILAN or D-A) utilized.

Many of the design options as listed in Table 2 have specific considerations that need to be understood when deciding how to run the design tool. Specifically, when looking at the operating temperature, different temperature regimes use different BOP components. Under ambient or room temperature operation, the BOP components would only have to be rated for the chosen operating temperature rather than the severe temperature operations needed for cryogenic operation. Thus, the

Table 2 – Model controls and results.

Operating Conditions	Pressure Vessel Designs	Heat Exchanger Designs	Results/Targets
Temperature variations: • Ambient (298 K) • Cold (200 to 298 K) • Cryogenic (< 200 K)	*Tank types:* • Type 1 metal (Al or SS) • Type 3 metal (Al or SS) + carbon fiber • Type 4 polymer + carbon fiber	*Internal Heat Exchangers Designs – HexCell:* • Hexagonal channels • Powder adsorbent • Dimensional and material thickness variations	*Total system values:* • Volume • Mass • H_2 storage • Estimate cost
Pressure variations: • Low pressure (< 10 MPa; Type 1 tanks) • High pressure (> 10 MPa; Type 3 and 4 tanks)	*Design dimensions:* • L-to-D ratio > 2:1 • Length and Diameter variations available	*Internal Heat Exchangers Designs – MATI:* • Calculate adsorbent storage volume vs. free H_2 volume • Compacted adsorbent	*System Capacity values:* • Volumetric Capacity (g_{H2}/L_{system}) • Gravimetric Capacity (g_{H2}/g_{sys})
Useable H2: • > 0.01 kg_{H2} • DOE LDV target of 5.6 $kg_{H2,useable}$	*Endcap design:* • Hemispherical (h = r) • Oblate (h = 2/3*r) • Elliptical (h = ½*r)	–	–

model automatically updates the mass, volume, and estimate cost of the BOP based on the operating temperature. Similar changes are implemented based on the operating pressure as well.

The PV and heat exchanger design options also have specific underlying calculations associated with each design decision. When designing a PV, the hoop stress and von mises stress are calculated based on the PV type (Type 1, 3, or 4), material selection, and dimensions, with wall thicknesses being used as the most conservative calculated PV. These wall thicknesses, in addition to the endcap selection, are then used to design the PV and calculate its mass and volume (internal and external). Note that additional design considerations, such as the use of insulation, are also added to the PV design based on the operating temperature. Similarly, the internal heat exchanger is created based on the adsorbent type (powder or compact), internal volume, and other specifications as designated by the user.

When all model parameters have been selected, the full adsorbent-based H_2 storage system is designed within the ASDT, and the complete system values can be calculated to obtain values such as the total system mass, system volume, and useable H_2 storage. Additional calculations are also performed to calculate the volumetric capacity and gravimetric capacity, which are both critical DOE Technical Targets [1].

Another output to consider that is outside the brevity of this paper is the estimated system cost. The following is the order of importance for impact of the model: system cost, volumetric capacity, and gravimetric capacity. Considering all possible permutations, the outputs of a parametric study that utilized the ASDT were in the order of billions [19]. This parametric study analyzed and optimized data so that the gravimetric and volumetric capacities were maximized while the system cost were minimized, which resulted in the two cyro-adsorbent H_2 storage system designs that were built into 2 L prototypes for the HSECoE: one powder MOF-5™ HexCell design, and one compacted MOF-5™ puck MATI design.

Results

Prototype validation

Several small-scale experiments were performed to validate the ASDT models, but the largest-scale validation of the model involved the 2 L H_2 storage prototypes built for the HSECoE. The prototype MATI cryo-adsorbent system was the primary method for validating the ASDT and had an internal capacity of 2 L that used compacted 0.4 g/cc density MOF-5™ pucks with no fillers/binders.

The prototype experimental setup was designed specifically with validation in mind. H_2 that was stored at room temperature enters the mass flow meter (MFM) to obtain reliable H_2 storage measurement. Still at room temperature, the H_2 flows from the MFM to the tubing coil in the liquid nitrogen bath. The bath is a heat exchanger that cools the room temperature H_2 flowing in the tubes to liquid nitrogen temperatures. After flowing through the coil, the H_2 flows to an insulated line from one liquid nitrogen bath to the prototype in the second liquid nitrogen bath. The liquid nitrogen bath is used to maintain the operating temperature of the prototype by providing a constant boundary condition for model validation. Because the 2 L prototype vessel is a flanged design that is quite different from the typical PVs used on LDVs, the model is only used to validate the internal chamber of the 2 L prototype. This includes the adsorbent material, internal tank components, and the H_2 within the prototype.

As shown in Fig. 5 from the 2016 DOE-EERE-FCTO AMR [16,35], various operation conditions were tested. The following variables were used to compare the experimentally calculated H_2 stored within the prototype with the model results:

- $H_{2,in}$ = total mass of hydrogen flowing through the MFM to fill the lines and be stored within the 2 L prototype.
- $m_{tube,tot}$ = total mass of hydrogen stored within the tubing as calculated by the pressure and temperature of the hydrogen within the tubing.

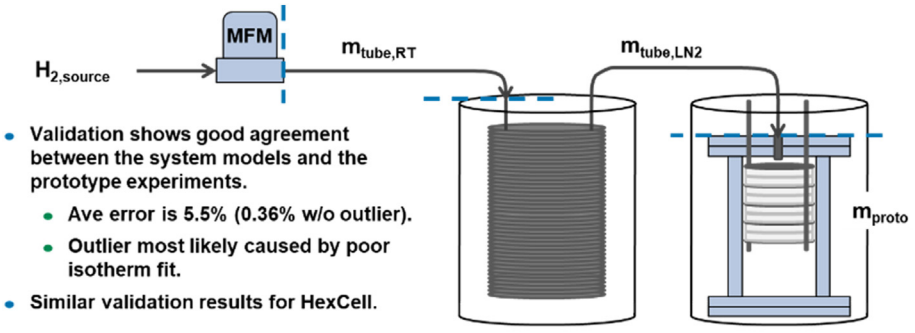

Op. Conditions	$H_{2,in}$	$m_{tube,tot}$	$m_{proto,exp}$	$m_{proto,model}$	%-Diff
(1.07 bar, 83.7 K) ➔ (60.0 bar, 91.3 K)	86.85 g	41.69 g	45.16 g	45.45 g	0.639%
(1.09 bar, 83.7 K) ➔ (100.0 bar, 84.5 K)	140.54 g	72.56 g	67.99 g	68.09 g	0.158%
(5.05 bar, 84.0 K) ➔ (60.5 bar, 106.6 K)	59.55 g	28.51 g	31.04 g	24.57 g	-20.86%
(5.23 bar, 83.2 K) ➔ (100.2 bar, 102.4 K)	107.24 g	58.10 g	49.14 g	49.00 g	-0.285%

Fig. 5 – Validation results of the MATI prototype illustrating accuracy of isotherm fitting.

- $m_{prototype,exp}$ = total mass of hydrogen stored within the 2 L prototype as calculated from the validation experiment.
- $m_{prototype,model}$ = total mass of hydrogen stored within the 2 L prototype as calculated from the computational model.

Validation experiments were run for various operating conditions, with the initial and final conditions held at equilibrium. Four of these validation runs are shown in Fig. 5. Out of the four cases shown, only one result was above ±1%, and this outlier was most likely caused by a poor isotherm fit.

Although there was a temperature gradient in the H_2 tubing between the MFM and the 2 L prototype from room temperature (22 °C) to liquid nitrogen temperature (77 °C), the H_2 within the tubing ($m_{tube,tot}$) was assumed to follow a step difference between room temperature and liquid nitrogen temperatures. The H_2 within the line in the liquid nitrogen bath is assumed to be at liquid nitrogen temperatures, with the H_2 between the MFM and the liquid nitrogen bath held at room temperature. The temperature inside the 2 L prototype was measured and used in the model calculations accordingly. Figs. 5 and 6 shows representative data from the MATI validation experiments.

An experimental validation was also performed for a 2 L prototype based on powder MOF-5™ and a HexCell internal heat exchanger. This HexCell validation showed similar results, proving the viability of the HexCell models. Note that these validation experiments are not shown here for the sake of brevity.

The purpose of these stand-alone adsorbent system models is to facilitate the design of a full-scale H_2 storage system for a LDV based on the adsorbent material as described by its H_2 adsorption isotherms. Fig. 6 shows how the validated system models are scaled up from the 2 L HexCell and MATI prototype validation experiments to the full-scale adsorbent

	Powder MOF-5 HexCell HX	Compact MOF-5 MATI HX
Measured 2-liter Prototype (material + $HX_{internal}$)	(90 K, 80 bar) ➔ (85 K, 1.7 bar)	(84.5 K, 100 bar) ➔ (83.7 K, 1.1 bar)
Gravimetric Capacity	0.112 g/g	0.092 g/g
Volumetric Capacity	23.6 g/l	37.2 g/l
Full-scale 5.6 kg System model (material + $HX_{internal}$)	(80 K, 100 bar) ➔ (160 K, 5.0 bar)	(80 K, 100 bar) ➔ (160 K, 5.0 bar)
Gravimetric Capacity	0.125 g/g	0.100 g/g
Volumetric Capacity	32.9 g/l	44.4 g/l
Full-scale 5.6 kg System model (full system)	(80 K, 100 bar) ➔ (160 K, 5.0 bar)	(80 K, 100 bar) ➔ (160 K, 5.0 bar)
Gravimetric Capacity	0.0321 g/g	0.0315 g/g
Volumetric Capacity	18.9 g/l	21.0 g/l

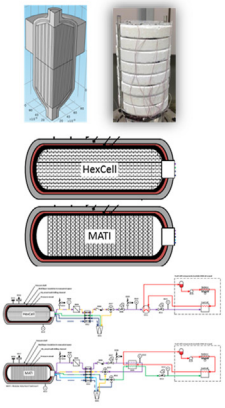

Fig. 6 – Scaling the validation results to obtain gravimetric and volumetric capacities.

H_2 storage systems. As referenced in Fig. 6, three variables were compared: operating conditions, gravimetric capacity, and volumetric conditions.

Three scales from 2 L prototype to full-scale LDV were compared for these sets of variables that include various control volumes. The first set (first three rows) validates the model by only including the 2 L prototype referenced in Fig. 5. The model matched within the predicted results with <1% error. The second set (middle three rows) uses the validated model to create a full-scale H_2 storage tank with a control volume of only the internal components within the tank, including the adsorbent, heat exchanger, and H_2. Finally, the third set (bottom three rows) shows the full-scale H_2 storage tank model expanded to include the full adsorbent H_2 storage system, which is made up of the tank internals (middle three rows of Fig. 6), the PV, MLVI, safety components, and the full BOP connecting the H_2 storage to the vehicle fuel cell.

Model sensitivity analysis/parametric analyses

An ideal adsorbent system given current technology has been theorized by Tamburello et al. [19], however, the system could not meet DOE's technical targets for gravimetric or volumetric capacity [1]. Although, it is expected that the data and system tools developed in the study may create further understanding of thermal transport optimization through the HexCell and MATI system designs, and future adsorbent materials research may be informed and thus meet or even exceed DOE's technical targets.

To illustrate the significance of selecting the appropriate isotherm fitting, the UNILAN and D-A computational models were analyzed separately for comparison of both gravimetric and volumetric capacity, as demonstrated in Fig. 7 for powder MOF-5™ at various temperature intervals. For both isotherm fittings, the volumetric capacity increases as tank pressure increases, and decreases as operating temperature increases. Above 10 MPa, the volumetric capacity reaches an asymptotic limit across all temperatures shown. This limit is linked to reduced excess H_2 (n_{ex,H_2}) stored compared to pure CcH_2 at elevated pressures combined with the increased tank wall thickness (mass) necessary for elevated pressures. The UNILAN volumetric capacity curve reached the 2020 DOE target at its lowest temperature condition.

For both isotherm fittings, the gravimetric capacity reached the 2020 DOE target at its lowest temperature condition. Both graphs have a maximum for each set of operating conditions, which is also a result of the balance between the decreased n_{ex,H_2} stored and increased tank wall thickness. However, the fittings display slightly different trends. The gravimetric capacity for the UNILAN fitting seems to maximize around 12 MPa across all operating temperatures, while D-A maximizes around 10 MPa. The UNILAN graph also increases steadily from 4 to 12 MPa, while the D-A graph has a small, steady increase.

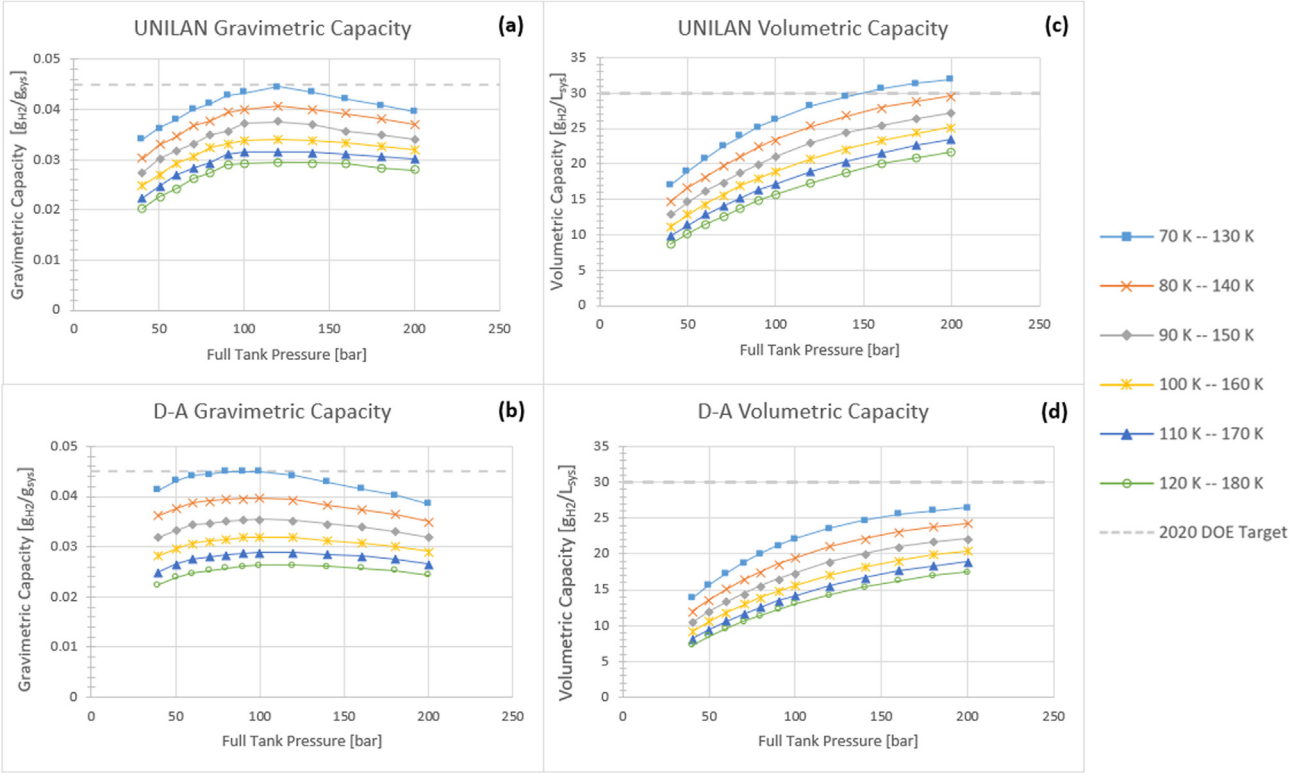

Fig. 7 – Trends of powder MOF-5™ HexCell with 2:1 L-to-D ratio aluminum Type 1 PVs: (a) UNILAN gravimetric capacity, (b) D-A gravimetric capacity, (c) UNILAN gravimetric capacity, (d) D-A volumetric capacity.

Conclusion

An ASDT was described to assist material developers in making estimates for initial design parameters for hydrogen storage systems by bridging the gap between initial hydrogen adsorption measurements and full-scale adsorbent hydrogen storage system estimates to address the DOE LDV technical targets [1]. These design parameters would be entered as inputs into a broader framework model that would estimate the performance of the H_2 storage system integrated with the fuel cell system to better estimate full-scale hydrogen storage vehicle performance. The utility was demonstrated by performing various analyses of potential adsorption-based H_2 storage systems for fuel cell vehicle applications and then down-selected adsorbent system designs based on validated experimental data from the HSECoE. Note that the ASDT results matched the prototype validation experimental data as well as the literature data for MOF-5™ adsorption [28].

The standalone ASDT describes the following sections: heat exchanger designs, computation models, prototype validation, and parametric analysis. The heat exchanger design options include the HexCell and MATI while varying compaction of the adsorbent. The D-A and UNILAN adsorption theories are two computation model options, and both are valid methods for modeling. However, based on the results of the prototype validation of the experimental MATI design comparison with the adsorption models, UNILAN may be the more versatile theory for modeling excess adsorption in H_2 storage applications. This observation is demonstrated through the parametric analysis where the volumetric and gravimetric capacities are plotted for both adsorption theories using the HexCell heat exchanger design. However, the choice of adsorption theory is primarily material dependent and should be verified using the actual experimental excess adsorption data.

Ultimately, this tool is meant to bridge the gap between the thermodynamic and kinetic data routinely captured by material developers and the data required to exercise the broader fuel cell LDV framework model. The current ASDT is specifically designed for LDV applications, although additional work is currently underway to expand its capabilities to medium and heavy-duty vehicles, as well as to other alternative applications such as stationary and portable power. Future versions of the ASDT may also include new adsorption models, such as the two-state Langmuir model, to better improve its applicability to a wider range of adsorbent material. Finally, design options for these models could also be extended to other gas-solid interactions such as pure methane and/or natural gas correlations to support the development and adoption of those technologies.

Declaration of competing interest

The authors declare that they have no known competing financial interests or personal relationships that could have appeared to influence the work reported in this paper.

Acknowledgements

This work was done at Savannah River National Laboratory, Pacific Northwest National Laboratory, and the National Renewable Energy Laboratory as part of the Hydrogen Storage System Modeling project, sponsored by the U.S. Department of Energy. Funding was provided by U.S. Department of Energy, Office of Energy Efficiency and Renewable Energy, Hydrogen Fuel Cell Technologies Office. The authors would like to thank our sponsors Jesse Adams and Ned Stetson for their outstanding support. Savannah River National Laboratory is operated by Battelle Savannah River Alliance, LLC, for the U.S. Department of Energy under Contract No. 89303321CEM000080. PNNL is operated by Battelle for DOE under contract DE-AC05-76RLO1830. The National Renewable Energy Laboratory is operated by Alliance for Sustainable Energy, LLC, for the U.S. Department of Energy under Contract No. DE-AC36-08GO28308. The U.S. Government retains and the publisher, by accepting the article for publication, acknowledges that the U.S. Government retains a nonexclusive, paid-up, irrevocable, worldwide license to publish or reproduce the published form of this work, or allow others to do so, for U.S. Government purposes.

REFERENCES

[1] DOE technical targets for onboard hydrogen storage for light-duty vehicles [Online]. Available: https://www.energy.gov/eere/fuelcells/doe-technical-targets-onboard-hydrogen-storage-light-duty-vehicles; 22 March 2021.
[2] Satypal S, Petrovic J, Read C, Thomas G, Ordaz G. The U.S. Department of energy's national hydrogen storage project: progress towards meeting hydrogen-powered vehicle requirements. Catalysis Today 2007;120:246–56.
[3] Ahluwalia R, Hua T, Peng J, Lasher S, McKenney K, Sinha J, Gardiner M. Technical assessment of cryo-compressed hydrogen storage tank systems for automotive applications. Int J Hydrogen Energy 2010;35:4171–84.
[4] Hardy BJ, Anton DL. Hierarchical methodology for modeling hydrogen storage systems. Part I: scoping models. Int J Hydrogen Energy 2009;34:2269–77.
[5] Hardy BJ, Anton DL. Hierarchical methodology for modeling hydrogen storage systems. Part II: detailed models. Int J Hydrogen Energy 2009;34:2992–3004.
[6] Garrison SL, Hardy BJ, Gorbounov MB, Tamburello DA, Corgnale C, van Hassel BA, Mosher DA, Anton DL. Optimization of internal heat exchangers for hydrogen storage tanks utilizing metal hydrides. Int J Hydrogen Energy 2012;37:2850–61.
[7] Mohan G, Prakash Maiya M, Srinivasa Murthy S. Performance simulation of metal hydride hydrogen storage device with embedded filter and heat exchanger tubes. Int J Hydrogen Energy 2007;32:4978–87.
[8] Botzung M, Chaudourne S, Gillia O, Perret C, Latroche M, Percheron-Guegan A, Marty P. Simulation and experimental validation of a hydrogen storage tank with metal hydride. Int J Hydrogen Energy 2008;33:98–104.
[9] Raju M, Ortmann JP, Kumar S. System simulation model for high-pressure metal hydride hydrogen storage systems. Int J Hydrogen Energy 2010;35:8742–54.

[10] Richard MA, Benard P, Chahine R. Gas adsorption process in activated carbon over a wide temperature range above the critical point. Part 2: conservation of mass and energy. Adsorption 2009;15:53–63.
[11] Richard MA, Benard P, Chahine R. Gas adsorption process in activated carbon over a wide temperature range above the critical point. Part I: modified Dubinin-Astakhov model. Adsorption 2009;15:43–51.
[12] Czerny AM, Benard P, Chahine R. Adsorption of nitrogen on granular activated carbon: experiment and modeling. Langmuir 2005;21:2871–5.
[13] Zhou W, Wu H, Hartman MR, Yildirim T. Hydrogen and methane adsorption in metal-organic frameworks: a high-pressure volumetric study. J Phys Chem C 2007;111:16131–7.
[14] Hardy B, Corgnale C, Chahine R, Richard MA, Garrison S, Tamburello D, Cossement D, Anton D. Modeling of adsorbent based hydrogen storage systems. Int J Hydrogen Energy 2012;37:5691–705.
[15] Hydrogen Storage Systems Modeling [Online]. Available: https://www.hymarc.org/models.html; 22 March 2021.
[16] Tamburello D, Hardy B, Sulic M, Anton D, Kesterson M, Corgnale C. Compact cyro-adsorbent hydrogen storage systems for fuel cell vehicles. In: ASME Power and Energy Conference. Lake Buena Vista, FL; June 24-28, 2018.
[17] Purewal J, Veenstra M, Tamburello D, Ahmed A, Matzger AJ, Wong-Foy AG, Seth S, Liu Y, Siegel DJ. Estimation of system-level hydrogen storage for metal-organic frameworks with high volumetric storage density. International Journal of Hydrogen Energy 2019;44(29):15135–45.
[18] Rozzi E, Demetrio Minuto F, Lanzini A. Dynamic modeling and thermal management of a Power-to-Power system with hydrogen storage in microporous adsorbent materials. Journal of Energy Storage 2021;41:102953.
[19] Tamburello DA, Hardy BJ, Corgnale C, Sulic M, Anton DL. Cyro-adsorbent hydrogen storage systems for fuel cell vehicles. In: ASME 2017 Fluids Engineering Division Summer Meeting. Hawaii: Waikoloa; 2017. July 31-August 3.
[20] Palla S, Kaisare NS. Evaluating the impact of pellet densification and graphite addition for design of on-board hydrogen storage in a fixed bed of MOF-5 pellets. International Journal of Hydrogen Energy 2020;45(48):25875–89.
[21] Zheng B, Gao K, Tian D, Yao W, Zhang L, Wang L, Wang J. Residual guest-assisted MOF-5 powder densification. Inorganic Chemistry 2021;60(17):13419–24.
[22] Samantaray SS, Putnam ST, Stadie NP. Volumetrics of hydrogen storage by physical adsorption. Inorganics 2021;9(6):45.
[23] Brooks KP, Sprik SJ, Tamburello DA, Thornton MJ. Design tool for estimating metal hydride storage system characteristics for light-duty hydrogen fuel cell vehicles. Int J Hydrogen Energy 2020;45:24917–27.
[24] Brooks KP, Sprik SJ, Tamburello DA, Thornton MJ. Design tool for estimating chemical hydrogen storage system characteristics for light-duty fuel cell vehicles. Int J Hydrogen Energy 2018;43:8846–58.
[25] Anton DL, Motyka T, Hardy BJ, Tamburello DA, Corgnale C. IV.B.1 hydrogen storage engineering Center of excellence. HSCoE; 2014.
[26] Bhatia SK, Myers AL. Optimum conditions for adsorptive storage. Langmuir 2006;22:1688–700.
[27] Xu C, Yang J, Veenstra M, Sudik A, Purewal JJ, Ming Y, Hardy BJ, Warner J, Maurer U, Siegel DJ. Hydrogen permeation and diffusion in densified MOF-5 pellets. Int J Hydrogen Energy 2013;38:3268–74.
[28] Purewal JJ, Liu D, Yang J, Sudik A, Siegel DJ, Maurer S, Muller U. Increased volumetric hydrogen uptake of MOF-5 by powder densification. Int J Hydrogen Energy 2012;37:2723–7.
[29] Richard MA, Cossement D, Chandonia PA, Chahine R, Mori D, Hirose K. Preliminary evaluation of the performance of an adsorption-based hydrogen storage system. AIChE Journal 2009;55:2985–96.
[30] Liu D, Purewal JJ, Yang J, Sudik A, Maurer S, Mueller U, Ni J, Siegel DJ. MOF-5 composites exhibiting improved thermal conductivity. Int J Hydrogen Energy 2012;37:6109–17.
[31] Juan-Juan J, Marco-Lozar JP, Suarez-Garcia F, Cazorla-Amoros D, Linares-Solano A. A comparison of hydrogen storage in activated carbons and a metal-organic framework (MOF-). Carbon 2010;48:2906–9.
[32] Marco-Lozar JP, Juan-Juan J, Suarez-Garcia F, Cazorla-Amoros D, Linares-Solano A. MOF-5 and activated carbons as adsorbents for gas storage. Int J Hydrogen Energy 2012;37:2370–81.
[33] Ahluwalia RK, Peng JK. Automotive hydrogen storage system using cryo-adsorption on activated carbon. Int J Hydrogen Energy 2009;34:5476–87.
[34] Myers AL, Monson PA. Adsorption in porous materials at high pressure: theory and experiment. Langmuir 2002;18(26):10261–73.
[35] Tamburello DA. Hydrogen storage modeling: public access, maintenance, and enhancements. DOE-EERE-FCTO AMR FY; 2016.

Acronyms

AMR: Annual Merit Review and Peer Evaluation
ASDT: Adsorbent System Design Tool
BOP: Balance of Plant
CcH_2: Cyro-Compressed Hydrogen
D-A: Dubinin-Astakhov isotherm model
DOE: Department of Energy
EERE: Energy Efficiency and Renewable Energy
FCTO: Fuel Cell Technology Office
H_2: Hydrogen
HSECoE: Hydrogen Storage Engineering Center of Excellence
LDV: Light-Duty Vehicle
MATI: Modular Adsorbent Tank Insert
MFM: Mass Flow Meter
MLVI: Multilayer Vacuum Insulation
MOF: Metal Organic Framework
PV: Pressure Vessel